Sec. 3. What we used was the crudest imaginable, and the error involved needs to be ascertained.[15a] Another approximation is that the response of the system to the perturbation that was used to determine the shielding was calculated only to first order in the perturbation. This lead to the result that the x, y, and z parts of $\mathbf{S}_l \cdot \mathbf{S}_{k'k}$ get shielded in precisely the same way. It can be shown however that this "degeneracy" in the "triplet potential" is removed in higher order. This is usually a relatively minor effect, but it is interesting to note the changes in the character of the results when the approximations are relaxed.

PHYSICAL REVIEW VOLUME 137, NUMBER 6A 15 MARCH 1965

Electronic Band Structure of TiC, TiN, and TiO†

V. ERN*
Laboratory for Insulation Research, Massachusetts Institute of Technology, Cambridge, Massachusetts
AND
A. C. SWITENDICK‡
Solid State and Molecular Theory Group, Massachusetts Institute of Technology, Cambridge, Massachusetts
(Received 26 October 1964)

The band structure of metallic face-centered cubic TiC, TiN, and TiO has been obtained by the augmented-plane-wave (APW) method at the equivalent of 256 points in the Brillouin zone and for an energy range appropriate to cover the nonmetal $2s$ and $2p$ and the titanium $3d$ and $4s$ states. A density of states, the Fermi energy, and contours of constant energy were obtained for the three compounds. A charge distribution in the APW scheme was derived from the equivalent of 32 points in the zone, and the admixture of the bands was analyzed. The results are consistent with the available experimental data.

INTRODUCTION

THE carbides, nitrides, and oxides of transition metals have been studied intensively in the past years. Face-centered cubic titanium carbide and nitride belong to the group of so-called hard refractory metals. Their high melting point, hardness, brittleness, and metallic conductivity are common to all carbides and nitrides of the Group IV and V transition metals.[1] Metallic TiO crystallizes in the rock salt structure when quenched from the melt or annealed and quenched from 950 to 1225°C. The structure stabilizes with about 15% vacancies on both atomic sites.[2–4] The melting point of TiO is close to that of titanium metal, but its hardness is comparable to that of TiC or TiN.

The binding in the hard metals is expected to arise from simultaneous contributions of metallic, covalent, and ionic bonding to the cohesive energy. The relative position and degree of admixture of the $2s$ and $2p$ metalloid levels with the d and s transition-metal states play a decisive role in the binding. Several models favoring metal-metal or metal-nonmetal interaction have been proposed[5–9] to account for the trends in the properties of these compounds. The orbital overlap and the character of the d band in the transition metal oxides have been analyzed by Morin[10,11] and Goodenough.[12] Other authors[9,13–15] have investigated the stability of the rock salt structure in the hard metals, in particular the vacancy problem in TiO.

Band-structure calculations using linear-combinations-of-atomic-orbitals (LCAO) methods have been made for some of these compounds: Bilz[9] has presented a model of band structure for the hard metals assuming (in the Slater and Koster[16] scheme) the values of the two-center integrals for the $3d$, $4s$, and $2p$ interactions.

† Sponsored by the U. S. Office of Naval Research and Air Force Materials Laboratory.
* Present address: Central Research Department, Experimental Station, E. I. DuPont de Nemours, Wilmington, Delaware.
‡ Present address: The Sandia Corporation, Albuquerque, New Mexico.
[1] For a review see, for example, R. Kieffer and F. Benesovsky, *Hartstoffe* (Springer-Verlag, Vienna, 1963).
[2] P. Ehrlich, Z. Elektrochem. **45**, 362 (1939); S. Anderson, B. Collén, U. Kuylenstierna, and A. Magnéli, Acta Chem. Scand. **11**, 1641 (1957).
[3] A. D. Pearson, J. Phys. Chem. Solids **5**, 316 (1958).
[4] S. P. Denker, Ph.D. thesis, Massachusetts Institute of Technology, 1963 (unpublished).
[5] Ya. S. Umanskii, Ann. Secteur Anal. Physicochim. Inst. Chim. Gen. (U.S.S.R.) **16**, No. 1, 127 (1943).
[6] E. Dempsey, Phil. Mag. **8**, 285 (1963).
[7] R. E. Rundle, Acta Cryst. **1**, 180 (1948).
[8] H. Krebs, Acta Cryst. **9**, 95 (1956).
[9] H. Bilz, Z. Physik **153**, 338 (1958).
[10] F. J. Morin, Bell System Tech. J. **37**, 1047 (1958).
[11] F. J. Morin, Phys. Rev. Letters **3**, 34 (1959); J. Appl. Phys. **32**, 2195 (1961).
[12] J. B. Goodenough, Phys. Rev. **117**, 1442 (1960).
[13] P. V. Geld and V. A. Ckaj, Zh. Strukt. Khim. **4**, 235 (1963).
[14] S. P. Denker, *Nuclear Metallurgy*, edited by J. T. Waber, P. Chiotti and W. N. Miner (Metallurgical Society of AIME, 1964), Vol. 10, p. 51.
[15] L. Kaufman and A. Sarney, Ref. 14, p. 267.
[16] J. C. Slater and G. F. Koster, Phys. Rev. **94**, 1498 (1954).

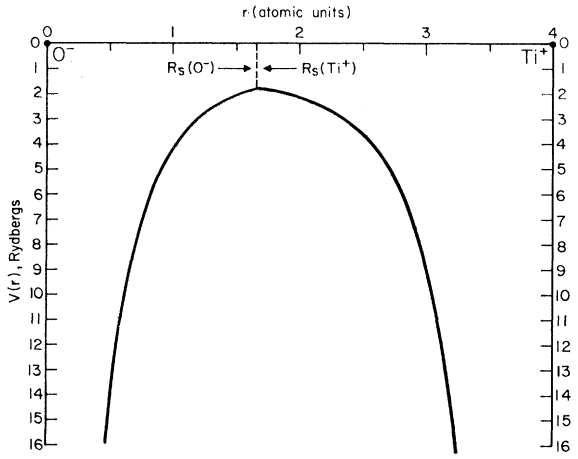

FIG. 1. Potential for TiO in the [100] direction.

Costa and Conte[17] computed a density of states in the $3d$ band of titanium for TiC and TiN, neglecting all but the d functions interaction. Yamashita[18] has obtained the eigenvalues at a few high-symmetry points in the zone for TiO and NiO by a modified tight-binding procedure with $3d$—$2p$ coupling.

The present band-structure calculation for TiC, TiN, and nondefective TiO was performed by the augmented-plane-wave (APW) method of Slater.[19] This method requires no *a priori* assumption on the degree of interaction between the different states. The results depend on the choice of the "muffin-tin" crystalline potential necessary to solve the one-electron Schrödinger equation within the scheme.

POTENTIALS

The APW method in its present form requires the knowledge of a starting one-electron potential spherically symmetric within spheres centered on the atomic sites and constant in between. This potential should resemble the one-electron potential due to the actual charge distribution in the crystal as closely as possible. An *a posteriori* comparison of the assumed starting electronic configuration with the charge distribution, as derived from the occupied states of the computed band structure, should give some indication of the degree of self-consistency achieved within the method. For compounds the choice of the starting potential is further complicated by the need for assuming some ionicity, that is, a possible transfer of charge between spheres of different types.

For the three compounds studied here the ionic character should increase from the carbide to the monoxide, i.e., with increasing electronegativity of the nonmetal atom. For the present band-structure calculation the potentials of the constituent atoms were obtained with the programs of Herman and Skillman[20] for the self-consistent solution of the Hartree-Fock-Slater equations. The self-consistency criterion was 0.001 Ry. For TiC and TiN the potential in the respective spheres was taken as that obtained from the neutral atomic configurations: $Ti(3d)^2(4s)^2$, $C(2s)^2(2p)^2$, and $N(2s)^2(2p)^3$. For TiO an ionicity of ± 1 was assumed with the configurations for $Ti^+(3d)^2(4s)$ and for $O^-(2s)^2(2p)^5$. The free ion potentials should be corrected by the Madelung electrostatic field in the structure; this will raise all the one-electron states in the cation, and lower those in the anion sphere.

The Madelung interaction constant assumes nonoverlapping, spherically symmetric charge distributions. To account for the charge overlap between the first nearest neighbors, the following procedure was adopted to obtain the potential in the sphere of a particular ion: The Coulomb part of the potential and the radial charge density of each of the neighboring ions were expanded around the center of the chosen ion by the standard procedure of Löwdin,[21] and the expansions spherically averaged. The s-like terms of the expansions were added[22] to the Coulomb potential and to the radial charge density of the central ion, respectively. The total potential $V^s(r)$ in each sphere was then obtained as the sum of the superposed Coulomb part and the exchange term derived from the total charge density by Slater's[23] free-electron approximation

$$V_{\text{exch}}(r) = -6\{(3/8\pi)\rho(r)\}^{1/3},$$

which was used for all the potentials throughout this work.

In practice only a limited number of neighbors must be considered in the superposition procedure, and $V^s(r)$ can be adequately corrected for the presence of the remaining ions. Considering 26 neighbors around an ion A ($6B$ at $a/2$, $12A$ at $\sqrt{2}a/2$ and $8B$ at $\sqrt{3}a/2$ in the rock salt structure AB of lattice constant a), the total superposed radial charge density in sphere A was found to increase at most by 0.2% near the sphere radius when the next shell of neighbors (6 ions A at distance a) was added. This being a negligible charge overlap, the rest of the ions were treated as point charges. The superposed potential $V^s(r)$ was then corrected by using the remainder R_m of the Madelung sum

$$\begin{aligned} V_{\text{Ti}^+}(r) &= V^s{}_{\text{Ti}^+}(r) + [2R_m/(a/2)], \\ V_{\text{O}^-}(r) &= V^s{}_{\text{O}^-}(r) - [2R_m/(a/2)], \end{aligned} \tag{1}$$

with

$$R_m \equiv \sum_{j=m+1}^{\infty} \frac{n_j(a/2)}{d_j} = 1.74756 - \sum_{j+1}^{m} \frac{n_j(a/2)}{d_j},$$

[17] P. Costa and R. R. Conte, Ref. 14, p. 3.
[18] J. Yamashita, J. Phys. Soc. Japan **18**, 1010 (1963).
[19] J. C. Slater, Phys. Rev. **51**, 846 (1937); **92**, 603 (1953); M. M. Saffren and J. C. Slater, *ibid.* **92**, 1126 (1953).
[20] F. Herman and S. Skillman, *Atomic Structure Calculations* (Prentice-Hall, Inc., Englewood Cliffs, New Jersey, 1963).
[21] Per-Olow Löwdin, Advan. Phys. **5**, 96 (1956).
[22] L. F. Mattheiss, Bull. Am. Phys. Soc. **8**, 222 (1963).
[23] J. C. Slater, Phys. Rev. **81**, 385 (1951).

TABLE I. Potentials in the Ti sphere used for the band-structure calculation of TiO.

r	$-V(r)$	r	$-V(r)$
0.00158	27721.9468	0.42339	39.9693
0.00316	13795.2100	0.43603	38.0122
0.00474	9152.4032	0.44867	36.1909
0.00632	6830.6796	0.46131	34.4939
0.00790	5437.4595	0.47394	32.9111
0.00948	4508.5430	0.49922	30.0520
0.01106	3844.9812	0.52450	27.5482
0.01264	3347.2952	0.54978	25.3447
0.01422	2960.2161	0.57505	23.3945
0.01580	2650.5793	0.60033	21.6581
0.01738	2397.2781	0.62561	20.1028
0.01896	2186.2391	0.56088	18.7018
0.02054	2007.7184	0.67616	17.4337
0.02212	1854.7538	0.70144	16.2809
0.02370	1722.2397	0.72672	15.2292
0.02528	1606.3452	0.75199	14.2667
0.02686	1504.1407	0.77727	13.3836
0.02844	1413.3465	0.80255	12.5718
0.03002	1332.1627	0.82782	11.8239
0.03160	1259.1492	0.85310	11.1339
0.03476	1133.1787	0.87838	10.4964
0.03792	1028.3811	0.90365	9.9065
0.04108	939.8705	0.92893	9.3600
0.04423	864.1549	0.95421	8.8533
0.04739	798.6729	0.97949	8.3826
0.05055	741.5028	1.00476	7.9452
0.05371	691.1750	1.03004	7.5382
0.05687	646.5463	1.05532	7.1591
0.06003	606.7146	1.08059	6.8055
0.06319	570.9583	1.10587	6.4755
0.06635	538.6934	1.13115	6.1671
0.06951	509.4426	1.15642	5.8786
0.07267	482.8116	1.18170	5.6075
0.07583	458.4722	1.20698	5.3552
0.07899	436.1488	1.23226	5.1171
0.08215	415.6084	1.25753	4.8986
0.08531	396.6523	1.28281	4.6999
0.08847	379.1105	1.30809	4.5186
0.09163	362.8361	1.33336	4.3480
0.09479	347.7019	1.35864	4.1872
0.10111	320.4247	1.38392	4.0358
0.10743	296.5432	1.40920	3.8931
0.11375	275.4842	1.43447	3.7585
0 12007	256.7933	1.45975	3.6315
0.12639	240.1063	1.48503	3.5116
0.13270	225.1280	1.51030	3.3984
0.13902	211.6172	1.53558	3.2915
0.14534	199.3752	1.56086	3.1904
0 15166	188.2372	1.58613	3.0949
0 15798	178.0655	1.61141	3.0046
0 16430	168.7443	1.63669	2.9193
0 17062	160.1755	1.66197	2.8387
0 17694	152.2756	1.68724	2.7625
0 18326	144.9729	1.71252	2.6906
0 18958	138.2057	1.73780	2.6227
0 19590	131.9206	1.76307	2.5586
0.20222	126.0706	1.78835	2.4982
0.20854	120.6149	1.81363	2.4412
0.21485	115.5175	1.83891	2.3876
0.22117	110.7464	1.86418	2.3372
0.23381	102.0736	1.88946	2.2898
0.24645	94.4043	1.91474	2.2453
0.25909	87.5844	1.94001	2.2035
0.27173	81.4887	1.96529	2.1645
0.28437	76.0142	1.99057	2.1280
0.29701	71.0760	2.04112	2.0622
0.30964	66.6031	2.09168	2.0053
0.32228	62.5369	2.14223	1.9566
0.33492	58.8261	2.19278	1.9155
0.34756	55.4298	2.24334	1.8812
0.36020	52.3118	2.29389	1.8533
0.37284	49.4417	2.34445	1.8313
0.38548	46.7932	2.39500	1.8148
0.39811	44.3441	2.44555	1.8034
0.41075	42.0751	2.49611	1.7968
	Potential for the titanium sphere in TiO.		
0.00221	7203.4026	0.27466	35.8812
0.00443	3588.7623	0.28331	34.2709
0.00664	2383.7533	0.29216	32.7686
0.00885	1781.1624	0.30102	31.3647
0.01107	1419.5462	0.30987	30.0508
0.01328	1178.4237	0.32758	27.6640
0.01549	1006.1591	0.34528	25.5570
0.01771	876.9352	0.36299	23.6880
0.01992	776.4082	0.38070	22.0228
0.02213	695.9716	0.39840	20.5326
0.02435	630.1489	0.41611	19.1932
0.02656	575.2884	0.43382	17.9842
0.02877	528.8623	0.45152	16.8884
0.03099	489.0646	0.46923	15.8911
0.03320	454.5710	0.48694	14.9800
0.03541	424.3881	0.50464	14.1448
0.03763	397.7563	0.52235	13.3765
0.03984	374.0845	0.54006	12.6677
0.04205	352.9061	0.55777	12.0121
0.04427	333.8479	0.57547	11.4040
0.04869	300.9374	0.59318	10.8389
0.05312	273.5257	0 61089	10.3127
0.05755	250.3458	0.62859	9.8217
0.06197	230.4939	0.64630	9.3629
0.06640	213.3059	0.66401	8.9336
0.07083	198.2837	0.69942	8.1538
0.07525	185.0459	0.73483	7.4659
0.07968	173.2959	0.77025	6.8567
0.08411	162.7993	0.80566	6.3153
0.08853	153.3685	0.84107	5.8328
0 09296	144.8513	0.87649	5.4016
0.09739	137.1234	0.91190	5.0155
0.10181	130.0816	0.94732	4.6689
0.10624	123.6404	0.98273	4.3573
0.11067	117.7274	1.01814	4.0766
0.11509	112.2812	1.05356	3.8234
0.11952	107.2508	1.08897	3.5946
0.12395	102.5905	1.12438	3.3877
0.12837	98.2622	1.15980	3.2002
0.13280	94.2323	1.19521	3.0304
0.14165	86.9555	1.23062	2.8762
0.15051	80.5674	1.26604	2.7362
0.15936	74.9184	1.30145	2.6091
0.16821	69.8904	1.33687	2.4935
0.17707	65.3889	1.37228	2.3884
0.18592	61.3374	1.40769	2.2930
0.19478	57.6737	1.44311	2.2062
0.20363	54.3463	1.47852	2.1275
0.21248	51.3125	1.51393	2.0560
0.22134	48.5364	1.54935	1.9913
0.23019	45.9880	1.58476	1.9327
0.23904	43.6415	1.62017	1.8799
0.24790	41.4752	1.65559	1.8324
0.25675	39.4701	1.69100	1.7899
0.26560	37.6101	1.72642	1.7519

where a is the lattice constant, n_j the number of neighbors at distance d_j from the central ion, and m the number of *different* distances taken in the superposition. The final potentials given by Eq. (1) agreed within 0.0015 Ry when m was changed from 3 to 4. Table I gives the potentials used for the Ti^+ and O^- spheres in the TiO band-structure calculation obtained by this procedure, with $m=3$.

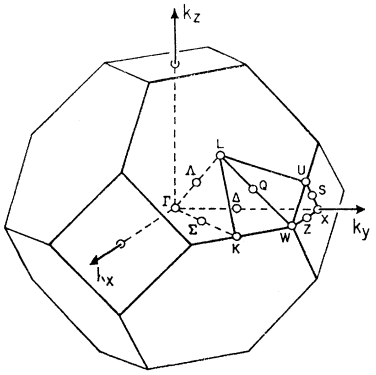

FIG. 2. Brillouin zone for the face-centered cubic lattice.

For the three compounds the APW sphere radii (R_s) were determined by requiring that the potentials be equal at the contact point of the two spheres around two nearest-neighbor atoms. The constant value V_c of the potential between the spheres was set equal to the common value at the spheres' surfaces. The experimental lattice constants were taken to be 4.326, 4.234, and 4.181 Å for TiC, TiN, and TiO, respectively.[3] Figure 1 shows the potential for TiO in the [100] direction. Table II summarizes the parameters used in the band-structure calculation.

TABLE II. Lattice constants, APW sphere radii, and constant part of the potentials used in band calculations; in atomic units (1 a.u. = 0.529 Å, 1 Ry = 13.605 eV).

	a (a.u.)	R_s (a.u.)	V_c (Ry)
TiC	8.1777	Ti: 2.2736; C: 1.8153	−1.355
TiN	8.0038	Ti: 2.2736; N: 1.7283	−1.355
TiO	7.9036	Ti^+: 2.3087; O^-: 1.6431	−1.845

METHOD OF COMPUTATION

The computational procedure used here for setting the matrix elements of the secular determinant is similar to that described by Wood.[24] For the more complicated NaCl structure[25] with two different atoms in the primitive cell, the plane-wave expansion is carried out around the different centers, and continuity with the atomic-like solution in each sphere is required. The potentials in the different spheres determine the respective solutions u_{lp} of the radial Schrödinger equation. The index p refers to the pth sphere in the primitive cell. The matrix elements (10) of Ref. 24 are now modified to

$$\langle\psi_i|H-E|R\psi_j\rangle=(\mathbf{k}_i\cdot R\mathbf{k}_j-E)$$
$$\times[\Omega\delta_{ij}-4\pi\sum_{p=1}^{\text{spheres}}R_{sp}^2\exp\{i(R\mathbf{k}_j-\mathbf{k}_i)\cdot\mathbf{d}_p\}$$
$$\times j_1(|R\mathbf{k}_j-\mathbf{k}_i|R_{sp})/R\mathbf{k}_j-\mathbf{k}_i|]+4\pi\sum_{p=1}^{\text{spheres}}R_{sp}^2$$
$$\times\exp\{i(R\mathbf{k}_j-\mathbf{k}_i)\cdot\mathbf{d}_p\}\sum_{l=0}^{\infty}(2l+1)P_l\left(\frac{\mathbf{k}_i\cdot R\mathbf{k}_i}{|\mathbf{k}_i||\mathbf{k}_j|}\right)$$
$$\times j_l(k_iR_{sp})j_l(k_jR_{sp})\frac{u_{lp}'(R_{sp};E)}{u_{lp}(R_{sp};E)},\qquad(2)$$

where the summation over p is carried over all the spheres in the primitive cell (2 for the present structure). R_{sp} is the APW sphere radius, and the vectors $\mathbf{d}_p$ appearing in the phase factors are from a coordinate origin to the center of the pth sphere. As before, $\mathbf{k}_i\equiv\mathbf{k}+\mathbf{K}_i$ ($\mathbf{K}_i$ being the reciprocal lattice vectors) is the set of selected vectors appropriate for each irreducible representation of the group of the wave vector $\mathbf{k}$ in the first zone. The elements of the secular determinant for a particular irreducible representation are then computed from

$$(H-E)_{ij}{}^{\alpha}=\sum_R\frac{G}{n_\alpha}[\Gamma_{jl}(R)]\langle\psi_i|H-E|R\psi_j\rangle.\qquad(3)$$

The rest of the notation follows that of Ref. 24.

RESULTS OF THE COMPUTATION

The computer-time requirements pose practical restrictions on the extent of the band-structure calculation. At any desired point in k space the bulk of the machine time is spent in setting the matrix elements (2) for the different irreducible representations of the group of the wave vector and in evaluating the determinants (3) in a prescribed mesh of energy. Keeping

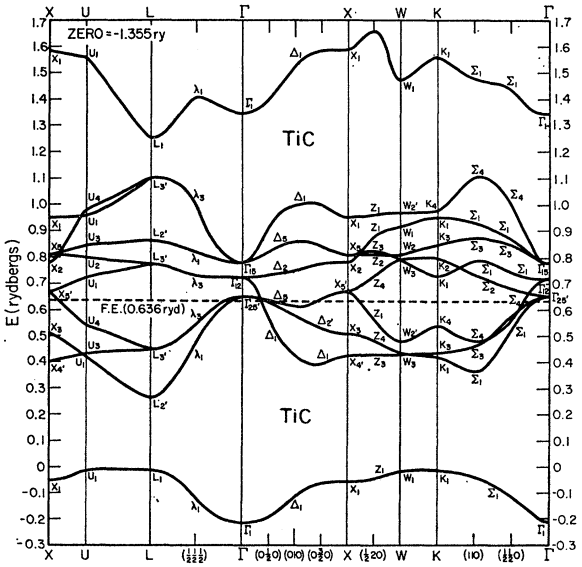

FIG. 3. Energy bands for TiC. Energies referred to a zero at −1.355 Ry, F. E. is the Fermi energy.

[24] J. H. Wood, Phys. Rev. **126**, 517 (1962).

[25] A. C. Switendick, Ph.D. thesis, Massachusetts Institute of Technology, 1963 (unpublished).

TABLE III. Calculated energies for TiC, TiN, and TiO at the equivalent of 32 points in the full zone. The values are referred to a zero at −1.355 Ry.

State	TiC	TiN	TiO
Γ_1	−0.210	−0.503	−1.073
	1.348	1.096	0.708
Γ_{15}	0.778	0.557	0.171
$\Gamma_{25'}$	0.651	0.653	0.556
Γ_{12}	0.722	0.728	0.705
X_1	−0.056	−0.416	−1.010
	0.953	0.881	0.818
	1.581		
$X_{4'}$	0.425	0.321	−0.039
		1.524	1.104
$X_{5'}$	0.671	0.492	0.130
X_2	0.777	0.786	0.807
X_3	0.510	0.507	0.305
X_5	0.804	0.815	0.842
L_1	−0.013	−0.362	−0.946
	1.253	1.209	0.785
$L_{2'}$	0.265	0.197	−0.160
	0.867	0.828	0.709
$L_{3'}$	0.453	0.354	0.035
	0.774	0.785	0.766
	1.11	1.029	0.978
W_1	−0.020	−0.391	−0.984
	0.913	0.862	0.820
	1.460		
W_2	0.804	0.828	0.852
$W_{2'}$	0.479	0.366	0.025
	0.964	0.936	0.920
W_3	0.436	0.354	0.007
	0.793	0.748	0.604
$\Delta_1(010)$	−0.113	−0.454	−1.015
	0.425	0.313	−0.037
	0.997	0.903	0.715
	1.523	1.322	0.983
$\Delta_{2'}(010)$	0.574	0.576	0.409
$\Delta_2(010)$	0.749	0.760	0.753
$\Delta_5(010)$	0.616	0.493	0.132
	0.858	0.795	0.741
$\Sigma_1(110)$	−0.022	−0.386	−0.972
	0.362	0.266	−0.087
	0.791	0.788	0.714
	0.924	0.873	0.805
	1.474	1.377	1.027
$\Sigma_2(110)$	0.732	0.743	0.706
$\Sigma_3(110)$	0.462	0.378	0.036
	0.872	0.792	0.628
$\Sigma_4(110)$	0.477	0.366	0.042
	1.11	1.020	0.969

the size of the secular equation within the limits necessary to achieve some prescribed accuracy in the eigenvalues saves considerable time. Several convergence tests indicated that restricting the list of $\mathbf{k}_i=\mathbf{k}+\mathbf{K}_i$ to all vectors with modulus $(48)^{1/2}(\pi/a) \leqslant |\mathbf{k}_i| \leqslant (80)^{1/2}(\pi/a)$ results in an accuracy ranging from 0.003 Ry at Γ to 0.01 Ry at the zone boundaries. At Γ this corresponds to an expansion up to the eighth-nearest neighbor in reciprocal space (an effective inclusion of 113 unsymmetrized plane waves). The expansion in spherical harmonics was taken up to $l=12$. No change in the eigenvalues was observed at Γ with an expansion up to $l=18$. The energy range was restructed to include the states derived from the Ti *3d* and 4*s*, and nonmetal 2*s* and 2*p* states. With the restrictions specified above, the $E(k)$ values for the three

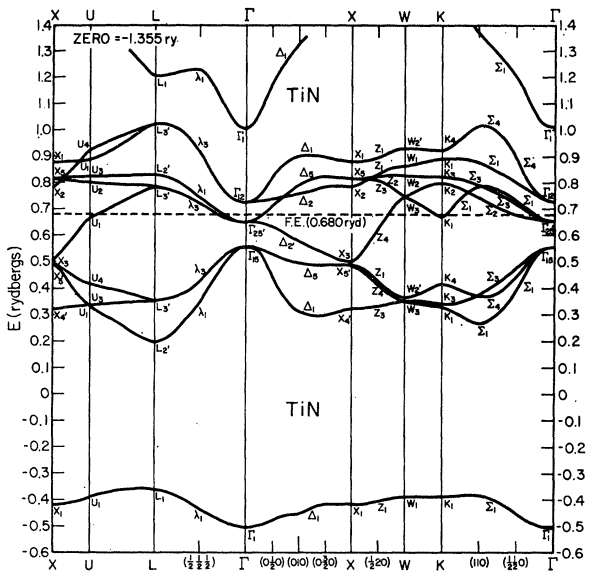

FIG. 4. Energy bands for TiN.

compounds were calculated[26] at the following points in the zone (Fig. 2): Γ(000), X(020), Δ($0\frac{1}{2}0$), Δ(010), Δ($0\frac{3}{2}0$), Z($\frac{1}{2}20$), W(120), K($\frac{3}{2}\frac{3}{2}0$), Σ(110), Σ($\frac{1}{2}\frac{1}{2}0$), λ($\frac{1}{2}\frac{1}{2}\frac{1}{2}$), and L(111). At U($\frac{1}{2}2\frac{1}{2}$) the eigenvalues are identical to K. Figures 3 through 5 show the energy dependence with k along the paths Γ-K-W-X [in the (001) plane] and Γ-L-U-X. The bands are drawn through the eigenvalues determined at the labeled points along the abscissa and using the appropriate compatibility relations. The **k** components are given in

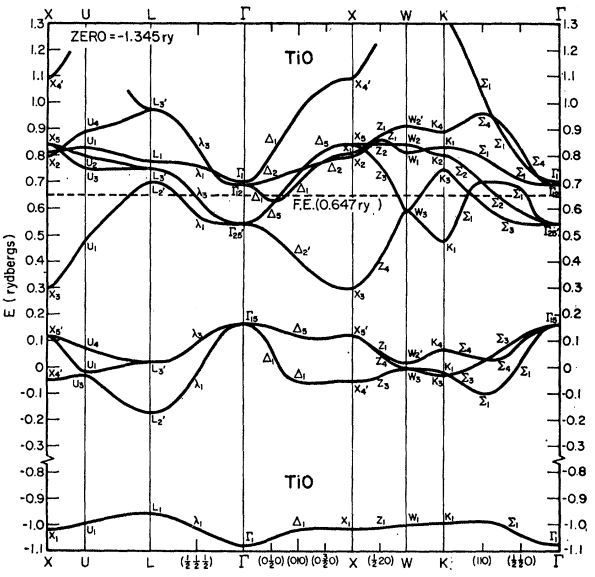

FIG. 5. Energy bands for TiO.

[26] This work was done in part using the facilities at the Computation Center at the Massachusetts Institute of Technology.

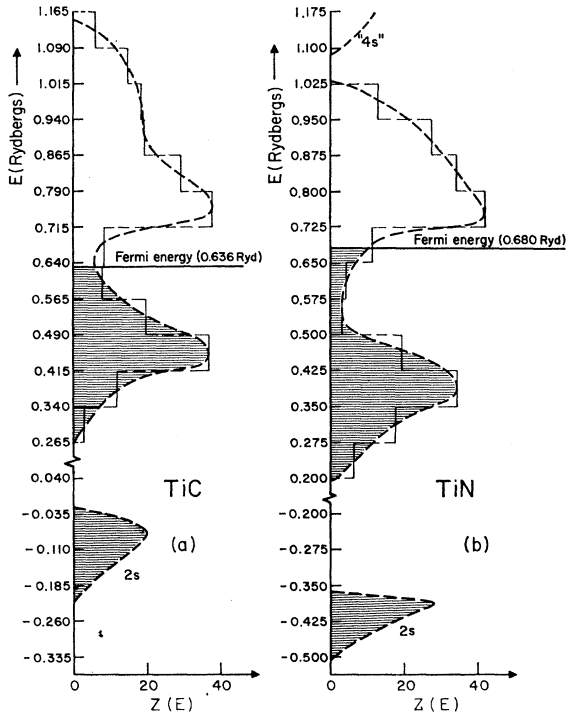

FIG. 6. Density-of-states histograms (spin included) for (a) TiC, (b) TiN, in electrons per primitive cell×Ry. Broken line schematic.

units of π/a. The standard notation of B.S.W.[27,28] for the different symmetry types has been used throughout this work. Table III gives the energy of states in the different bands for the subset of the equivalent of 32 high-symmetry points in the zone. These points uniformly cover the k space on a cubic grid of dimension π/a.

For a fairly stable density-of-states histogram a coverage of at least 256 uniformly distributed points in the zone (on a cubic mesh of side $\pi/2a$) is necessary. This requires, in addition to the states obtained, the eigenvalues at the points: $(\frac{1}{2}10)$, $(\frac{1}{2}\frac{3}{2}0)$, $(1\frac{3}{2}0)$, $(\frac{1}{2}1\frac{1}{2})$, $(\frac{1}{2}\frac{3}{2}\frac{1}{2})$, $(11\frac{1}{2})$, and $Q(1\frac{3}{2}\frac{1}{2})$, for which the group of the wave vector contains only two operations, and correspondingly large, computer-time-consuming, secular equations should be solved. For TiC and TiN these states were obtained by a graphical interpolation from the previously known energies. Whenever possible an average from different directions was taken. Several of the points were checked on the computer. The agreement ranged from 0.01 to 0.05 Ry, the best being for bands near the Fermi level. For TiO all of these states were obtained on the computer with a convergence to 0.02 to 0.03 Ry. For some points this required solving secular equations of the order of 32×32. The density-of-states curves were obtained by partitioning[29] the energy scale in equal intervals of width ΔE and counting the number of states in each interval for the 256 points in the full zone. Each state was weighted according to degeneracy and for both spin-up and -down occupancy. Different intervals ΔE were tried, and for each interval the partitions displaced along the energy scale in steps of $\frac{1}{3}\Delta E$. The most stable histograms were obtained for ΔE between 0.06 to 0.09 Ry. Figures 6 and 7 show the density of states for the three compounds for $\Delta E=0.075$ Ry. The Fermi energy was obtained as follows: Starting from the nonmetal $2s$ band, the available states were filled for TiC, TiN, and TiO, with 8, 9, and 10 electrons per primitive cell, respectively. In the present mesh this corresponds to filling 1024, 1152, and 1280 doubly occupied states. The next lower states (about 2.5 Ry below the Fermi level for TiC) is the narrow filled Ti $3p$ band.

The following qualitative features (cf. Figs. 6 and 7) were reproducible in all histograms. For the first two compounds the conduction band presents two broad humps corresponding to bonding and antibonding mixtures of the $2p$–$3d$ bands (cf. Figs. 3 and 4). The Fermi level lies near a minimum for TiC, and on the rising portion of the density of states for TiN. For the monoxide the density of states of the $3d$ bands still rises at the Fermi level, reaching a maximum at about 2 eV above the Fermi energy. At the Fermi level the

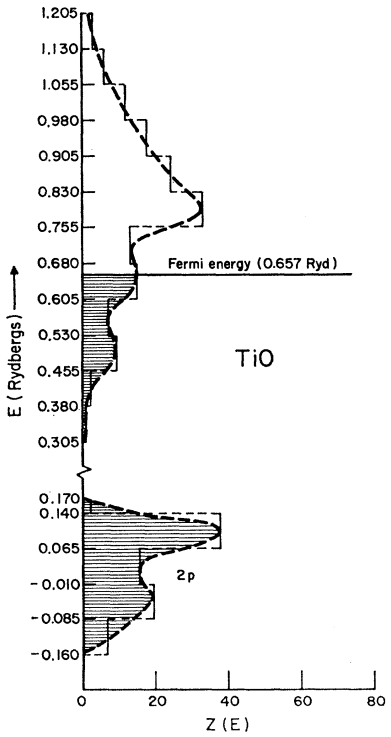

FIG. 7. Density-of-states histogram (spin included) for TiO (electrons/primitive cell×Ry). $2s$ band omitted.

[27] L. P. Bouckaert, R. Smoluchowski, and E. Wigner, Phys. Rev. **50**, 58 (1963).

[28] H. Jones, *The Theory of Brillouin Zones and Electronic State in Crystals* (North-Holland Publishing Company, Amsterdam, 1960).

[29] G. A. Burdick, Phys. Rev. **129**, 138 (1963).

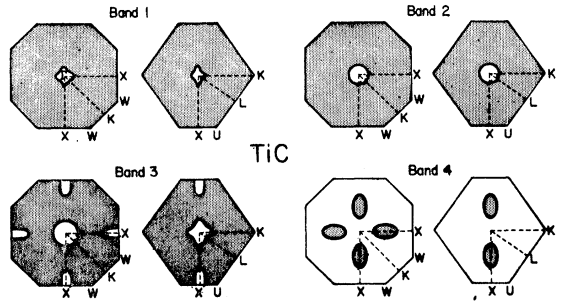

FIG. 8. Contours in k space at the Fermi level for TiC. Distance Γ-X=0.77 (a.u.)$^{-1}$. Shaded regions filled with electrons.

density of states is 0.4 to 0.5 electrons per primitive cell-eV for TiC and about 1 for TiN and TiO. Costa and Conte[17] found values of 0.23 and 0.49 from low-temperature specific-heat and magnetic-susceptibility measurements, respectively, for TiC. The superconducting transition temperature is reported higher for TiN than for TiC,[1] in agreement, according to the BCS formula,[30] with the trends derived for the density-of-states curves assuming a similar pair-interaction constant for the two compounds. The Debye temperature is reported slightly lower for TiN than for TiC.[31]

Some qualitative information about the intersections of the Fermi surface with symmetry planes in the zone, as given by the present APW calculation, seemed worthwhile in the hope that these orbits may help in interpreting the de Haas–van Alphen or magnetoresistance experiments when these data become available for the three materials studied here. Figures 8 through 10 give the contours of constant energy at the Fermi level in the (001) and (110) planes through Γ. The orbits are drawn in the reduced zone scheme through the marked $\mathbf{k}$ points as determined graphically from the computed APW states. Band 1 refers to the first not-completely-filled zone.

For TiC, pockets of holes occur in the first three bands. Piper[32] has proposed a simple mixed-conductivity two-band model to explain the temperature dependence of the Hall coefficient for TiC.

CHARGE DISTRIBUTION

If $E_n(\mathbf{k})\equiv E$ is a particular eigenvalue in the nth band, the APW crystal function can be written in a compact form, as

$$\psi\mathbf{k}=\alpha\sum_i A_i{}^n e^{(i\mathbf{k}_i\cdot\mathbf{r})}+\sum_{p=1}^{\text{spheres}}\beta_p e^{(i\mathbf{k}\cdot\mathbf{d}_p)}\times\sum_{l=0}^{\infty}\sum_{m=-l}^{+l}B_{lm}{}^p\frac{u_{lp}(r_p;E)}{u_{lp}(R_{sp};E)}Y_l{}^m(\theta_p\varphi_p),$$

with

$$B_{lm}{}^p\equiv\sum_i A_i{}^n C_{lm}{}^P(\mathbf{k}_i),$$

where $\mathbf{k}_i\equiv\mathbf{k}+\mathbf{K}_i$, $A_i{}^n$ are the components of the APW eigenvector determined from the secular equation, $Y_l{}^m(\theta_p,\varphi_p)$ the normalized spherical harmonics for the pth sphere, $C_{lm}{}^P(\mathbf{k}_i)$ the APW matching coefficients at each sphere surface,[24,25] and $u_{lp}(r_p;E)$ the solutions of the radial Schrödinger equation for the energy E in the pth sphere. α is defined as zero within the sphere and 1 between them; β_p is 1 in the pth sphere and zero elsewhere.

If $\Psi_\mathbf{k}$ is normalized over the volume of the Wigner-Seit cell, one obtains

$$1=\frac{1}{N}\int_{\text{cell}}\psi_\mathbf{k}{}^*\psi_\mathbf{k}{}^d=\frac{1}{N}\sum_{i,j}A_i{}^nA_j{}^n\int_{\text{outside spheres}}e^{i(\mathbf{k}_i-\mathbf{k}_i)\cdot\mathbf{r}}d\tau+\sum_{p=1}^{\text{spheres}}\sum_{l=0}^{\infty}\int_0^{R_{sp}}P_{lp}{}^2(r_p)dr_p,\quad(4)$$

where $\sqrt{N}$ is the normalization constant, and the functions

$$P_{lp}{}^2(r_p)\equiv\frac{1}{N}\sum_{m=-l}^{+l}|B_{lm}{}^P|^2\frac{u_{lp}{}^2(r_p;E)}{u_{lp}{}^2(R_{sp};E)}r_p{}^2$$

can be interpreted as the spherically averaged radial charge densities for a given l in the pth sphere. The number of electronic charges in a given sphere is

$$Q^p=\sum_{l=0}^{\infty}q_l{}^p\equiv 2\sum_{l=0}^{\infty}\int_0^{R_{sp}}P_{lp}{}^2(r_p)dr_p,$$

and in the plane-wave region

$$Q^{\text{P.W.}}=\frac{2}{N}\sum_{i,j}A_i{}^nA_j{}^n\int_{\text{outside spheres}}e^{i(\mathbf{k}_i-\mathbf{k}_j)\cdot\mathbf{r}}d\tau,$$

the factor 2 deriving from the double occupancy of each Bloch state. As before, previous symmetrization[24] simplifies the problem.

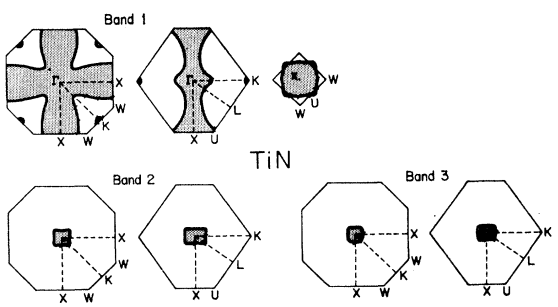

FIG. 9. Contours in k space at the Fermi level for TiN. Distance Γ-X=0.78 (a.u.)$^{-1}$. Shaded region filled with electrons.

[30] J. Bardeen, L. N. Cooper, and J. R. Schrieffer, Phys. Rev. **108**, 1175 (1957).
[31] C. R. Houska, J. Phys. Chem. Solids **25**, 359 (1964).
[32] J. Piper, Ref. 14, p. 29.

TABLE IV. Number of valence electrons in the APW spheres and in the intermediate region in the Wigner-Seitz cell. "Valence" includes 2*s* states for the nonmetal spheres. The states are labeled following the atomic notation according to *l* and the number of nodes of the radial part of the wave function in a given sphere. "Bands" refer to the charge distribution given by the average on the occupied states at the 32 points in the full zone (Table III). Atomic or ionic refers to the valence electrons of the free atom or ion in the same spherical volume for the configurations Ti: $(3d)^2(4s)_6^2$, C: $(2s)^2(2p)^2$, N: $(2s)^2(2p)^3$, Ti^+: $(3d)^2(4s)$, and $O^-(2s)^2(2p)^5$.

TiC						TiN						TiO					
In Ti sphere			In C sphere			In Ti sphere			In N sphere			In Ti^+ sphere			In O^- sphere		
state	bands	atomic	state	bands	atomic	state	bands	atomic	state	bands	atomic	state	bands	ionic	state	bands	ionic
3*d*	2.36	1.78	2*s*	1.19	1.44	3*d*	1.90	1.78	2*s*	1.51	1.61	3*d*	1.78	1.80	2*s*	1.54	1.69
4*s*	0.17	0.32	2*p*	1.81	1.26	4*s*	0.14	0.32	2*p*	3.20	2.21	4*s*	0.16	0.21	2*p*	3.70	3.59
4*p*	0.26	···	3*d*	0.02	···	4*p*	0.27	···	3*d*	0.02	···	4*p*	0.36	···	3*d*	0.03	···
4*f*	0.03	···				4*f*	0.05	···				4*f*	0.09	···			
	2.82	2.10		3.02	2.70		2.36	2.10		4.73	3.82		2.39	2.01		5.27	5.22
														2.86[a]			5.45[a]
	In plane waves: 2.16						In plane waves: 1.90						In plane waves: 2.31				

[a] After the charge superposition procedure previously described. Obtained by subtracting from the total superposed charge, the 1*s* atomic core charge in the O^- sphere, and the atomic core up to 3*p* (17.93 electrons) in the Ti^+ sphere. The core states are considered to be localized in the spheres.

Table IV gives the number of valence electrons in the APW spheres and in the plane-wave region, obtained from the average of the filled state at the equivalent of 32 points in the zone (Table III). A comparison with the free atomic or ionic charge in the same spherical volume is made. The pictorial description obtained for TiC is that of positive spheres of approximately +1 charge with 2 electronic charges in the intermediate region of each cell. Figure 11 shows the components and the total radial charge density $P_p^2(r) \cong \sum_{l=0}^{3} P_{lp}^2(r)$ for the two spheres in TiO, obtained from the average of the filled states of Table III. A comparison is made with the initial-valence (see footnote of Table IV) radial charge density.

Reasonable agreement exists between the starting and the derived charges for the C and O^- spheres. The nitrogen sphere contains approximately one extra electronic charge in 2*p* states, indicating that some intermediate ionicity should have been assumed for a more consistent charge distribution. In the Ti spheres 4*p*- and 4*f*-like functions became important. Their contribution is specially noticeable at the sphere radius where higher *l* components can drastically affect the behavior of the wave function. The 4*p* function is responsible for the "hump" in the radial charge density at $r=0.88$ a.u.

The 3*d* radial function has a more diffuse (bonding) character than does a free atom *d* function. The same was found true for the 2*p* functions in TiC and to a lesser degree in TiN. An analysis of all the computer states at $\Delta(010)$ in the 2*p*–3*d* bands of TiC showed a progressively localized (antibonding) character of the functions for the high-energy empty states. Similar behavior was found by Wood[33] for the 3*d* functions in iron. Tables V through VII give the percentage of charge contained in the APW spheres from the different spherical harmonics (up to $l=3$) for the filled states of Table III, including the empty states at $\Delta(010)$. For each point in *k* space the states are ordered in increasing energies starting from the nonmetal 25 band (Figs. 3 to 5). The amount in the plane-wave region can be obtained approximately as the complement to the sum of the given percentages for each state [cf. Eq. (4)].

Because of the strong mixing in the bands, only a fit of the pure t_{2g} symmetry (*xy* type) 3*d* bands was attempted with the LCAO scheme.[16] Fitting in the nearest-neighbor approximation for the states Γ_{25}', Δ_2',

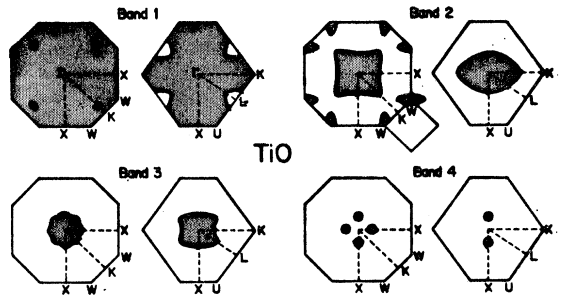

FIG. 10. Contours in *k* space at the Fermi level for TiO. Distance Γ-$X=0.79$ (a.u.)$^{-1}$. Shaded regions filled with electrons.

TABLE V. Analysis of the charge in the APW spheres for TiC (percent).

	In C sphere				In Ti sphere			
State	2*s*	2*p*	3*d*	4*f*	4*s*	4*p*	3*d*	4*f*
Γ_1	50.5		0.00		13.8		0.00	
X_1	60.7		0.00		1.7		16.6	
X_4'		42.2		0.05		15.5		0.03
X_3			2.2				68.1	
L_1	65.0		0.1			9.5		0.8
L_2'		29.6		0.1	10.2		20.1	
L_3'		33.8		0.1			48.3	
W_1	63.0		0.01	0.01		2.6	13.9	0.3
W_2'		40.5	0.00	0.04	4.1		34.0	0.7
W_3		30.4	0.5	0.05		9.0	23.0	0.04
Σ_1	55.9	0.4	0.1	0.00	4.5	5.8	3.5	0.6
Σ_1	2.4	32.5	0.03	0.04	6.2	0.2	27.5	0.4
Σ_3'		27.0	0.6	0.07		5.9	33.7	0.2
Σ_4		36.5	0.02	0.08		0.4	46.3	0.3
Δ_1	54.6	0.7	0.03	0.00	8.1	3.2	2.5	0.1
Δ_1	2.1	36.1	0.1	0.02	2.6	1.2	33.0	0.6
Δ_2'			1.9	0.04			73.7	0.2
Δ_5		33.1	0.3	0.1		3.3	41.6	1.1
Δ_2			2.31	0.01			91.9	0.05
Δ_5		39.2	0.1	0.05		2.0	48.3	1.4
Δ_1	12.3	16.3	0.5	0.2	2.8	0.1	54.3	1.1
Δ_1	4.2	31.5	0.1	0.01	11.9	2.4	4.6	0.7

[33] J. H. Wood, Phys. Rev. **117**, 714 (1960).

TABLE VI. Analysis of the charge in the APW spheres for TiN (percent).

State	In N sphere 2s	2p	3d	4f	In Ti sphere 4s	4p	3d	4f
Γ_1	67.4		0.00		9.2		0.00	
Γ_{15}		81.6		0.00		1.9		3.1
$\Gamma_{25'}$			1.3				84.2	
X_1	75.3		0.00		1.0		8.5	
$X_{4'}$		54.7		0.03		13.2		0.00
$X_{5'}$		73.4		0.00		6.0		1.7
X_3			1.9				69.1	
L_1	77.5		0.01			6.5		0.8
$L_{2'}$		39.8		0.02	9.9		14.9	
$L_{3'}$		49.4		0.1			33.0	
W_1	76.7		0.00	0.00		2.0	6.6	0.3
W_3		47.5	0.2	0.02		9.1	12.4	0.1
$W_{2'}$		55.6	0.00	0.02	3.7		20.6	0.7
Σ_1	75.4	0.1	0.01	0.00	1.3	4.3	2.1	0.5
Σ_1	0.8	45.4	0.02	0.02	6.8	0.4	17.4	0.4
Σ_4		52.7	0.01	0.06		0.3	30.5	0.3
Σ_3		46.7	0.3	0.03		6.1	19.3	0.3
Δ_1	72.1	0.1	0.00	0.00	4.0	2.4	1.9	0.2
Δ_1	1.2	49.9	0.04	0.01	3.6	1.4	19.5	0.6
Δ_5		64.1	0.1	0.03		3.7	12.1	1.7
$\Delta_{2'}$			1.7	0.02			74.9	0.2
Δ_2			2.1	0.00			92.2	0.1
Δ_5		15.7	0.2	0.1		0.2	76.9	0.5
Δ_1	8.9	8.8	0.5	0.2	3.7	0.2	65.9	0.5
Δ_1	10.9	29.4	0.03	0.00	11.6	3.4	7.0	0.3

X_3, X_5, and Σ_2 gave the following parameters for the energy integrals:

	$-E_{xy,xy}(110)$	$E_{xy,xy}(011)$	$E_{xy,xz}(011)$
TiC	0.381 eV	0.120 eV	0.134 eV
TiN	0.401 eV	0.124 eV	0.155 eV
TiO	0.715 eV	0.213 eV	0.220 eV

The values for TiC and TiN are close to the corresponding integrals calculated by Costa and Conte.[17] In the two-center approximation[16] the eigenvalues were best fitted by the following $(dd\sigma)$, $(dd\pi)$, and $(dd\delta)$ two-center integrals: −0.51, 0.25, and −0.02 eV for TiC; −0.52, 0.28, and −0.03 eV for TiN; −0.90, 0.44, and −0.05 eV for TiO.

COMPARISON WITH X-RAY DATA

The $K\beta_5$ emission band observed in transition metals is usually attributed to the transitions to the 1s levels from the 3d band hybridized with 4s and 4p functions.[34] Blokhin and Shuvaev[35] made a comparative study of K-emission spectra of TiO, TiN, and TiC. For TiO they find a weak $K\beta_5'$ line in coincidence with the usual Ti $K\beta_5$ line and two other bands lying, respectively, −5.8 eV ($K\beta_5$) and −21 eV[36] ($K\beta''$) below that line. The band calculation for TiO gives the position of the maxima of the density of states for the 2p- and 2s-like bands approximately as −5.1 and 20.8 eV, respectively, below the middle of the filled portion of the 3d conduction band (Figs. 7 and 12). The width of the $K\beta_5$ line (4.36 eV) agrees with the computed width (4.5 eV) of the 2p bands. Further agreement exists between the $K\beta_5$-$K\beta''$ distances as measured by several investigators[35,37] for TiC and TiN and the respective separation of the (2s) and (3d+2p) filled maxima in the density of states of Fig. 6. The comparison is as follows:

	$K\beta_5$-$K\beta''$ [35]	$K\beta_5$-$K\beta''$ [37]	Density of states
TiC:	7.0 eV	7.0 eV	7.1 eV
TiN:	10.0 eV	11.0 eV	10.7 eV

The long-wave K-absorption band[38] found in TiC re-

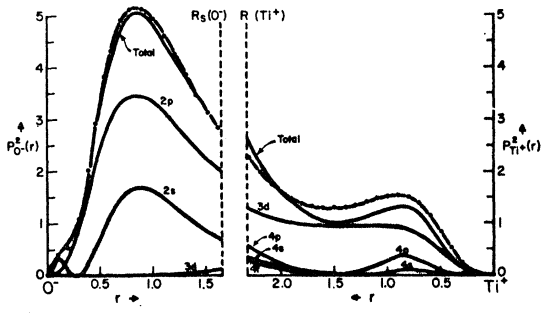

FIG. 11. Radial charge densities in the two spheres of TiO from the filled states at 32 points in the zone (———— from average of bands at 32 points; -·-·-·-·- charge density).

TABLE VII. Analysis of the charge in the APW spheres for TiO (percent).

State	In O sphere 2s	2p	3d	4f	In Ti sphere 4s	4p	3d	4f
Γ_1	71.5		0.00		8.4		0.00	
Γ_{15}		79.4		0.00		2.1		3.8
$\Gamma_{25'}$			1.8				76.4	
X_1	78.7		0.00		0.9		5.9	
$X_{4'}$		52.4		0.03		16.0		0.00
$X_{5'}$		70.2		0.03		7.1		2.1
X_3			2.1				56.6	
L_1	77.1		0.00			9.5		1.0
$L_{2'}$		40.9		0.02	11.7		10.1	
$L_{3'}$		59.6		0.05			20.3	
W_1	78.6		0.01	0.00		3.4	4.4	0.3
W_3		50.6	0.1	0.02		11.7	6.1	0.2
$W_{2'}$		61.5	0.00	0.00	4.5		11.2	1.0
W_3		16.2	1.0	0.1		0.07	57.3	1.6
Σ_1	76.6	0.02	0.00	0.00	1.0	6.8	1.4	0.7
Σ_1	0.5	47.8	0.02	0.02	8.7	0.8	10.1	0.5
Σ_3		53.6	0.2	0.02		8.1	9.5	0.5
Σ_4		62.5	0.00	0.02		0.5	18.0	0.4
Σ_3		20.5	0.8	0.1		0.2	52.6	2.0
Δ_1	74.5	0.02	0.01	0.00	3.8	3.9	1.4	0.3
Δ_1	0.9	52.8	0.01	0.00	5.3	2.3	10.0	0.9
Δ_5		70.3	0.04	0.02		4.5	3.8	2.4
$\Delta_{2'}$			2.0	0.03			61.8	0.7
Δ_1	20.6[a]	2.0	0.4	0.1	11.4	1.6	32.2	0.4
Δ_5		5.9	0.5	0.1		0.1	81.3	0.6
Δ_2			2.4	0.01			89.9	0.2
Δ_1	1.6[a]	25.5	0.24	0.02	3.5	4.0	45.1	0.06

[a] 3s character.

[34] W. W. Beeman and H. Freedman, Phys. Rev. **50**, 150 (1939); D. E. Bedo and D. H. Tomboulian, *ibid.* **113**, 464 (1959).

[35] M. A. Blokhin and A. T. Shuvaev, Bull. Acad. Sci. U.S.S.R., Phys. Ser. **26**, 429 (1962).

[36] Obtained graphically from Fig. 1 of Ref. 35.

[37] E. E. Vainshtein and V. I. Chirkov, Dokl. Akad. Nauk SSSR **145**, 1031 (1962) [English transl.: Soviet Phys.—Doklady **7**, 724 (1963)]; E. A. Shurakovskii and E. E. Vainshtein, *ibid.* **129**, 1269 (1959) [English transl.: *ibid.* **4**, 1308 (1960)].

[38] E. E. Vainshtein *et al.*, Dokl. Akad. Nauk SSSR **122**, 365 (1958) [English transl.: Soviet Phys.—Doklady **3**, 960 (1958)].

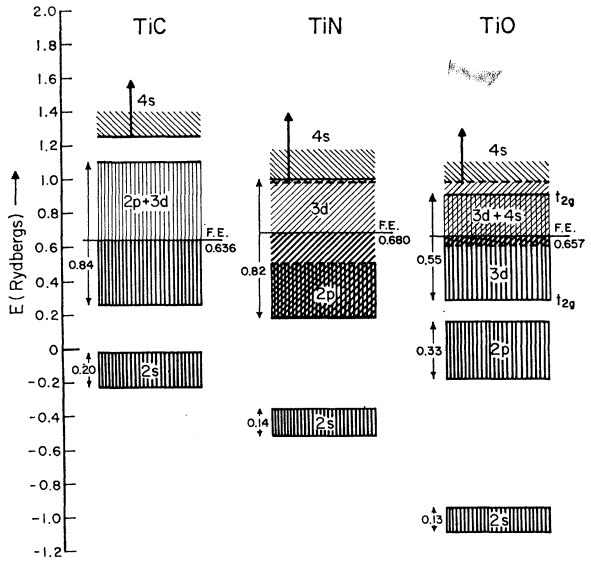

FIG. 12. Schematic trends in the band structures of TiC, TiN, and TiO. Labels indicate the predominant character of the band. The t_{2g} lines mark the width of the $3d$ band of that symmetry in the Δ direction.

sembles the empty portion of the density of states of Fig. 6(a). The higher intensity of the $K\beta''$ line for TiC[37] may correspond to an enhanced transition probability because of a stronger hybridization of the $2s$ band in the carbide (Tables V–VII). L and M spectra will be of great aid in assessing the present interpretation of the K-emission data.

The experimental shifts toward longer wavelengths of the $K\beta''$ and $K\beta_5$ lines for TiC and TiN relative to the respective lines for TiO [35] compare with the corresponding shifts of the maxima in the computer density of states:

	$K\beta_5$	$2p+3d$	$K\beta''$	$2s$
TiC:	+4.4 eV	+4.8 eV	+12.6 eV	+13.3 eV
TiN:	+2.0 eV	+3.9 eV	+6.3 eV	+8.9 eV

The discrepancy for the nitride would indicate that the $2s$ and $2p$ bands should be about 2–3 eV lower than predicted, giving a picture more closely resembling that for TiO. This is consistent with the discrepancy between the initial and derived charges in the nitrogen sphere (Table IV).

Denker[4] has measured the optical reflectivity on a single crystal of TiO and on an arc-melted polycrystalline sample of TiO. Companion and Wyatt[39] measured diffuse reflectance spectra from $TiO_{1.09}$ powder. Kramers-Kronig analysis[40] on Denker's data on TiO seem to indicate that interband transitions are responsible for the kink in reflectivity at about 2 eV and a plasma effect for the big drop in reflectivity at 3.8 eV. Figure 5 shows several filled and empty bands of almost parallel slope and about 2 eV separation, which could be responsible for the observed transition (like $\Sigma_1 \rightarrow \Sigma_4$, $\Sigma_3 \rightarrow \Sigma_1$, $\Delta_5 \rightarrow \Delta_1$, $\lambda_3 \rightarrow \lambda_1$, λ_3).

SUMMARY

The results of Table IV and the comparison with the x-ray emission data tend to indicate that a fairly correct position of the nonmetal $2p$ and $2s$ levels with respect to the titanium $3d$ band has been obtained by the present band calculation, at least for TiC and TiO. For TiN some intermediate ionicity should have been assumed for the starting potential. Figure 12 summarizes the relative position and the widths of the bands for the three compounds. The Γ_1–$\Gamma_1(2s$–$4s)$ interaction pushes the titanium $4s$-like band toward the higher energies above the $3d$ bands. With increasing nuclear charge of the nonmetal atom, the $2s$ band becomes more localized, and a corresponding lowering of the upper Γ_1 state occurs. For TiO the upper portion of the d band is strongly hybridized with $4s$ states. A calculation for a hypothetical face-centered cubic Ti metal without the nonmetal atoms gave the eigenvalues in the usual order Γ_1, Γ_{25}', Γ_{12} found in $3d$ transition metals. The hybridization of the $2s$ band with titanium states and the $3d$–$2p$ (metal–nonmetal) interaction decrease in the sequence from the carbide to the monoxide. The metal–metal $3d$ interaction is strong for the three compounds. The existence of a wide $3d$ band for these compounds of Ti, as given by the present one-electron picture agrees with the predictions of several authors[9–12] and with previous LCAO computations.[17,18]

ACKNOWLEDGMENTS

The authors areg reatly indebted to Professor Arthur von Hippel for the continuous support given to this work and to the Solid-State and Molecular Theory Group of MIT for many helpful discussions.

[39] A. L. Companion and R. E. Wyatt, J. Phys. Chem. Solids 24, 1025 (1963).

[40] S. P. Denker, Columbia University (private communication). We are greatly indebted to Professor D. J. Epstein, at M.I.T., for many helpful discussions on these data.

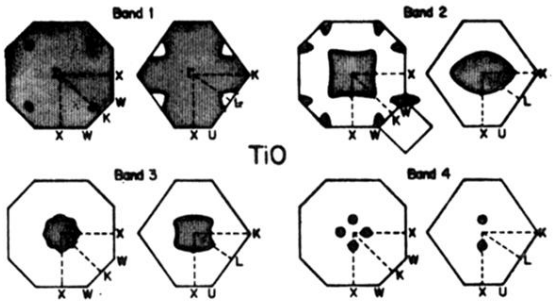

FIG. 10. Contours in k space at the Fermi level for TiO. Distance Γ-$X=0.79$ (a.u.)$^{-1}$. Shaded regions filled with electrons.

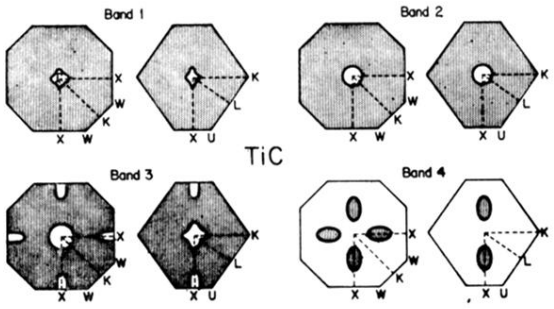

FIG. 8. Contours in k space at the Fermi level for TiC. Distance Γ-X=0.77 (a.u.)$^{-1}$. Shaded regions filled with electrons.